Acta Mech 224, 1045–1060 (2013)
DOI 10.1007/s00707-012-0800-3

Y. Kiani · M. R. Eslami

Instability of heated circular FGM plates on a partial Winkler-type foundation

Received: 27 September 2012 / Published online: 11 January 2013

Abstract Thermal buckling analysis of a transversely graded circular plate attached to a centric partial elastic foundation is studied, analytically. Thermomechanical properties of the circular plate are distributed across the thickness based on a power law function. The governing equations of the plate are obtained by means of the classical plate theory. A conventional Winkler-type foundation is assumed to be in contact with the plate which acts in compression as well as in tension. Proper boundary conditions are chosen after pre-buckling analysis of the plate, and stability equations are established via the adjacent equilibrium criterion. To analyze the thermal stability problem, the plate is divided into two sections, a foundation-less domain and an in-contact region. An exact procedure is presented to accurately predict the critical buckling temperature as well as the buckled configuration of the plate. Analysis of various involved parameters including the Winkler parameter, foundation radius, power law index, and loading type is presented. It is concluded that while the loading is symmetric, in many cases, the buckled configuration of the plate is asymmetric.

1 Introduction

As one of the frequently used structural elements, circular plates have been the subject of many researches for a long time. A literature survey shows the existence of numerous works on thermal/mechanical buckling of circular plates. Wang and his co-authors [1–4] presented the mechanical buckling analysis of plates considering various effects on plates. Axisymmetric buckling analysis of a Mindlin plate supported on a middle ring support [1], axisymmetric buckling of thick plates over a complete Winkler elastic foundation [2], and the effect of non-ideal boundary condition on stability of thin and Mindlin-type plates [3,4] are some topics discussed analytically. Also, Wang and his co-authors [3,5–7] covered other main topics in their research. For instance, simultaneous effects of a complete annular crack and Winkler elastic foundation [5], partial elastic foundation effect on the stability analysis of a thin plate [6], asymmetrical buckling analysis of a plate located on an intermediate elastic ring support [3], and existence of asymmetrical buckling configurations with the onset of symmetrical loading for a plate supported on a Winkler foundation [7] are reported in their research. Motivated by [1–7], Rao and Rao established the asymmetrical buckling analysis of a circular plate with elastically restrained edge and elastic ring supports [8,9]. In all of these works [1–9], the authors have presented analytical solutions to study the buckling problem of circular plates considering various effects when the loading type is uniform compression.

When buckling points of structures are extracted through the post-buckling paths, the nonlinear equilibrium equations have to be solved. Among the post-buckling analyses of circular plates, only few considered asymmetrical deformations for the plate, that is, the governing equations of the plate are established when displacements are functions of radial parameters only. Due to the geometrically nonlinear path of the plate,

Y. Kiani · M. R. Eslami (✉)
Mechanical Engineering Department, Academy of Sciences, Amirkabir University of Technology, Tehran, Iran
E-mail: eslami@aut.ac.ir

most of these works seem to employ a numerical method. For a class of these investigations, one may see the works reported in [10–14].

Due to their advantages over composites, especially when thermal effects are included, in recent years the functionally graded materials have attracted increasing attention in literature. Both the thermal buckling analysis and the mechanical buckling analysis of an FGM circular plate are of interest. The primary investigations on thermal and mechanical buckling analysis of circular plates are reported by Najafizadeh and Eslami [15,16]. In these works, the thin plate theory of Kirchhoff is assumed to obtain the partial differential equations of equilibrium. Stability equations are established and eigenvalue analysis is performed to analyze the stability problem of a circular plate. After that, Najafizadeh and Heydari [17,18] extended the same problem to the stability analysis of thick plates based on Reddy's third-order plate theory.

Some works are reported on stability analysis of Levy-type sectorial or annular sectorial plates by Saidi and his co-authors. Some of these works cover the mechanical buckling [19–21] and thermal buckling [22]. As we show later, the real state of an FG plate with at least one simply supported boundary conditions is not of the bifurcation type, and therefore, linearizing the problem in the stability equation is questionable.

Furthermore, Jalali and Naei [23] presented the buckling of moderately thick circular FG plates when the thickness of the plate is non-uniform. Stability equations of the plate are obtained in terms of Chebyshev polynomials, and pre-buckling analysis is done using the shooting method. A shooting method-based thermo-mechanical post-buckling analysis of circular FG plates is reported by Ma and Wang [24,25]. Most recently, Sepahi et al. [26] obtained the nonlinear equilibrium paths of a radially graded annular plate under the action of in-plane thermal loads. This analysis is limited to the case of symmetrical behavior of the plate. Imperfection sensitivity of a transversely graded thin FG plate under the action of nonlinear temperature distribution is done by Li et al. [27] based on a numerical shooting method.

Thermal buckling analyses of circular plates in contact with elastic foundation are limited in number, and all of them are restricted to the complete foundation condition. In this work, an exact analytical procedure is presented to predict the critical buckling temperature as well as the buckled configuration of a circular plate attached to a partially centric circular Winkler-type elastic medium. A conventional type of foundation is considered, which acts the same in compression and tension. Each thermomechanical property of the FG plate follows a power law form of the property distribution. The classical plate theory and von Karman type of geometrical nonlinearity are adopted to establish the governing equilibrium equations via the static version of virtual displacements. After a linear pre-buckling analysis, proper edge conditions are chosen to assure the occurrence of the bifurcation the phenomenon. The stability equations are obtained following the adjacent equilibrium criterion. The plate is divided into two sections, and for each one, the exact solution is obtained. Imposing the boundary and continuity conditions on the two regions yields a system of homogeneous algebraic equations which has to be treated as an eigenvalue problem to find the critical buckling load and the associated buckled shape. Effects of each involved parameter, such as power law index, loading type, contact domain, and elastic foundation coefficient, are discussed in detail.

2 Governing equations

Consider a thin solid circular plate made of FGMs of thickness h and radii a, referred to by the polar coordinates (r, θ, z), resting over a partial elastic foundation, as shown in Fig. 1. The elastic foundation is in contact with the plate only in the region $0 \leq r \leq b$. The material properties of the FG plate are assumed to be graded in thickness direction following the power law form for distribution of the constituent materials (ceramic and metal). The ceramic volume fraction V_c is assumed in the form [15–22]

$$V_c = \left(\frac{1}{2} + \frac{z}{h}\right)^k, \quad V_m = 1 - V_c \tag{1}$$

Following Voigt's rule, each property of the FG plate such as P may be described as a function of constituents' properties and volume fractions as

$$P(z) = P_m + P_{cm}\left(\frac{1}{2} + \frac{z}{h}\right)^k, \quad P_{cm} = P_c - P_m, \tag{2}$$

where P_m and P_c are the corresponding properties of the metal and ceramic, respectively, and k is a nonnegative constant called the power law index and shows the sharpness of the property dispersion. In the present work,

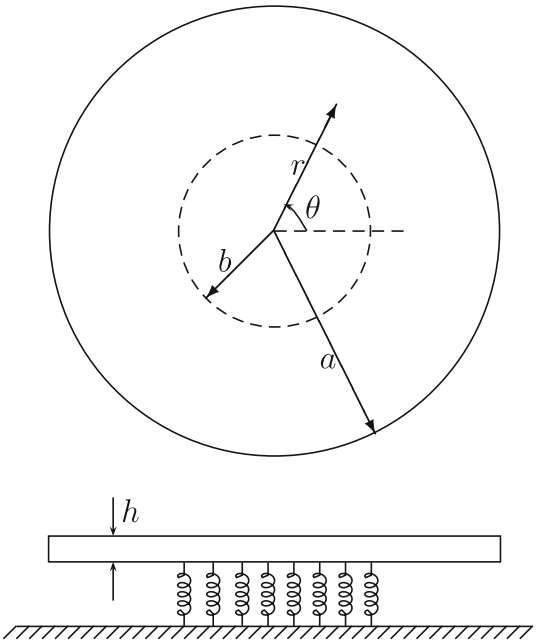

Fig. 1 Coordinate system and geometry for a thin circular FG plate supported by a partial Winkler foundation

we assume that the modulus of elasticity E, thermal conductivity K, and the thermal expansion coefficient α are described by Eq. (2), while Poisson's ratio ν is considered to be constant across the thickness [15–22].

Based on the von Karman assumptions, suitable for moderately large class of rotations, the nonlinear strain-displacement relations in polar coordinates may be written as [15,16]

$$\begin{aligned}
\varepsilon_{rr} &= u_{,r} + \frac{1}{2}w_{,r}^2, \\
\varepsilon_{\theta\theta} &= \frac{1}{r}v_{,\theta} + \frac{1}{r}u + \frac{1}{2r^2}w_{,\theta}^2, \\
\gamma_{r\theta} &= \frac{1}{r}u_{,\theta} + v_{,r} - \frac{1}{r}v + \frac{1}{r}w_{,\theta}w_{,r}.
\end{aligned} \tag{3}$$

Here, ε_{rr} and $\varepsilon_{\theta\theta}$ are the normal strains and $\gamma_{r\theta}$ is the shear strain, and a comma indicates partial derivative.

The classical theory of plates, based on Kirchhoff's assumptions, is adopted in the present work which estimates the displacements of an arbitrary point (u, v, w) in terms of middle surface displacements (u_0, v_0, w_0) as [15,16]

$$\begin{aligned}
u(r,\theta,z) &= u_0(r,\theta) - zw_{0,r}(r,\theta), \\
v(r,\theta,z) &= v_0(r,\theta) - \frac{z}{r}w_{0,\theta}(r,\theta), \\
w(r,\theta,z) &= w_0(r,\theta).
\end{aligned} \tag{4}$$

Within the framework of linear thermoelasticity of a continuum medium, the stress–strain relation is written as [28]

$$\begin{Bmatrix} \sigma_{rr} \\ \sigma_{\theta\theta} \\ \tau_{r\theta} \end{Bmatrix} = \frac{E}{1-\nu^2}\begin{bmatrix} 1 & \nu & 0 \\ \nu & 1 & 0 \\ 0 & 0 & \dfrac{1-\nu}{2} \end{bmatrix}\left(\begin{Bmatrix} \varepsilon_{rr} \\ \varepsilon_{\theta\theta} \\ \gamma_{r\theta} \end{Bmatrix} - (T-T_0)\begin{Bmatrix} \alpha \\ \alpha \\ 0 \end{Bmatrix}\right), \tag{5}$$

where T and T_0 are the temperature distribution through the plate and the reference temperature, respectively.

The stress resultants, based on the classical plate theory, are related to the stress tensor components as follows [16,17]:

$$
\begin{aligned}
(N_{rr}, N_{\theta\theta}, N_{r\theta}) &= \int_{-\frac{h}{2}}^{\frac{h}{2}} (\sigma_{rr}, \sigma_{\theta\theta}, \tau_{r\theta}) \mathrm{d}z, \\
(M_{rr}, M_{\theta\theta}, M_{r\theta}) &= \int_{-\frac{h}{2}}^{\frac{h}{2}} z(\sigma_{rr}, \sigma_{\theta\theta}, \tau_{r\theta}) \mathrm{d}z.
\end{aligned}
\tag{6}
$$

Substituting Eqs. (3)–(5) into Eq. (6) gives the stress resultants in terms of the mid-plane displacements as

$$
\begin{Bmatrix} N_{rr} \\ N_{\theta\theta} \\ N_{r\theta} \\ M_{rr} \\ M_{\theta\theta} \\ M_{r\theta} \end{Bmatrix} = \frac{1}{1-\nu^2} \times \begin{bmatrix} E_1 & \nu E_1 & 0 & E_2 & \nu E_2 & 0 \\ \nu E_1 & E_1 & 0 & \nu E_2 & E_2 & 0 \\ 0 & 0 & \frac{1-\nu}{2} E_1 & 0 & 0 & \frac{1-\nu}{2} E_2 \\ E_2 & \nu E_2 & 0 & E_3 & \nu E_3 & 0 \\ \nu E_2 & E_2 & 0 & \nu E_3 & E_3 & 0 \\ 0 & 0 & \frac{1-\nu}{2} E_2 & 0 & 0 & \frac{1-\nu}{2} E_3 \end{bmatrix}
$$
$$
\times \begin{Bmatrix} u_{0,r} + \frac{1}{2} w_{0,r}^2 \\ \frac{1}{r} v_{0,\theta} + \frac{1}{r} u_0 + \frac{1}{2r^2} w_{0,\theta}^2 \\ \frac{1}{r} u_{0,\theta} + v_{0,r} - \frac{1}{r} v_0 + \frac{1}{r} w_{0,r} w_{0,\theta} \\ -w_{0,rr} \\ -\frac{1}{r^2} w_{0,\theta\theta} - \frac{1}{r} w_{0,r} \\ -\frac{2}{r} w_{0,r\theta} + \frac{2}{r^2} w_{0,\theta} \end{Bmatrix} - \begin{Bmatrix} N^T \\ N^T \\ 0 \\ M^T \\ M^T \\ 0 \end{Bmatrix},
\tag{7}
$$

where N^T and M^T are the thermal force and thermal moment resultants, and E_1, E_2, and E_3 are constants to be calculated as

$$
\begin{aligned}
E_1 &= \int_{-\frac{h}{2}}^{\frac{h}{2}} E(z) \mathrm{d}z = h \left(E_m + \frac{E_{cm}}{k+1} \right), \\
E_2 &= \int_{-\frac{h}{2}}^{\frac{h}{2}} z E(z) \mathrm{d}z = h^2 E_{cm} \left(\frac{1}{k+2} - \frac{1}{2k+2} \right), \\
E_3 &= \int_{-\frac{h}{2}}^{\frac{h}{2}} z^2 E(z) \mathrm{d}z = h^3 \left(\frac{1}{12} E_m + E_{cm} \left(\frac{1}{k+3} - \frac{1}{k+2} + \frac{1}{4k+4} \right) \right),
\end{aligned}
\tag{8}
$$

$$
N^T = \frac{1}{1-\nu} \int_{-\frac{h}{2}}^{\frac{h}{2}} E(z) \alpha(z) (T - T_0) \mathrm{d}z,
$$

$$
M^T = \frac{1}{1-\nu} \int_{-\frac{h}{2}}^{\frac{h}{2}} z E(z) \alpha(z) (T - T_0) \mathrm{d}z.
$$

The equilibrium equations of a circular FGM plate on a partial elastic foundation under thermal loadings may be established on the basis of a static version of a virtual displacements method [29]. The total virtual potential energy of the plate, δV, is equal to the sum of total virtual strain energy of the plate and virtual strain energy of the elastic foundation as

$$\delta V = \int_0^a \int_0^{2\pi} \int_{-\frac{h}{2}}^{\frac{h}{2}} (\sigma_{rr}\delta\varepsilon_{rr} + \sigma_{\theta\theta}\delta\varepsilon_{\theta\theta} + \tau_{r\theta}\delta\gamma_{r\theta})\, r\mathrm{d}z\mathrm{d}\theta\mathrm{d}r + \int_0^a \int_0^{2\pi} H(r-b)K_w w_0 \delta w_0 r\mathrm{d}r\mathrm{d}\theta. \tag{9}$$

Here, H is the Heaviside step function. $H(r-b) = 1$ for $0 \le r < b$ and $H(r-b) = 0$ for $b < r \le a$. Also, K_w stands for the stiffness of the foundation.

Recalling Eqs. (7) and (8) and integrating the displacement gradients by parts to relieve the virtual displacements [29] and performing some mathematical simplifications to omit the common terms, expressions for the equilibrium equations of the FGM plate are obtained as follows:

$$\begin{aligned}
&\delta u_0 : N_{rr,r} + \frac{1}{r}N_{r\theta,\theta} + \frac{1}{r}(N_{rr} - N_{\theta\theta}) = 0,\\
&\delta v_0 : N_{r\theta,r} + \frac{2}{r}N_{r\theta} + \frac{1}{r}N_{\theta\theta,\theta} = 0,\\
&\delta w_0 : M_{rr,rr} + \frac{2}{r}M_{rr,r} + \frac{1}{r^2}M_{\theta\theta,\theta\theta} - \frac{1}{r}M_{\theta\theta,r} + \frac{2}{r}M_{r\theta,r\theta} + \frac{2}{r^2}M_{r\theta,\theta} + N_{rr}w_{0,rr}\\
&\quad + N_{\theta\theta}\left(\frac{1}{r^2}w_{0,\theta\theta} + \frac{1}{r}w_{0,r}\right) + 2N_{r\theta}\left(\frac{1}{r}w_{0,r\theta} - \frac{1}{r^2}w_{0,\theta}\right) - K_w w_0 H(r-b) = 0.
\end{aligned} \tag{10}$$

3 Existence of bifurcation-type buckling

In the previous section, the equilibrium equations are derived for a partially in-contact circular FGM plate. A pre-buckling analysis of the plate has to be studied to assure the existence of a primary–secondary equilibrium path. Assuming that bifurcation-type buckling occurs in the plate, the pre-buckling state of the plate is revealed when the equilibrium equations are rewritten and nonlinear terms are omitted from Eq. (7) [30].

For any type of boundary conditions, to produce in-plane thermal loads, immovability and periodicity conditions have to be satisfied. Neglecting the lateral deflection of the plate in pre-buckling state and solving the symmetrical type of the equilibrium equations yield

$$u_0^0(r,\theta) = 0. \tag{11}$$

Here, a superscript 0 indicates the pre-buckling configuration. Now, by means of Eq. (7), the following pre-buckling forces are obtained:

$$N_{rr}^0 = N_{\theta\theta}^0 = -N^T, \quad N_{r\theta}^0 = 0. \tag{12}$$

While the in-plane force resultants are obtained, extra pre-buckling moments exist which are equal to

$$M_{rr}^0 = M_{\theta\theta}^0 = -M^T, \quad M_{r\theta}^0 = 0. \tag{13}$$

As is observed from Eq. (13), due to the stretching–bending coupling of FG plates (or non-coincidence of mid-plane and neutral plane of the plate), even for the case of uniform temperature rise loading, initiation of thermal loading causes thermal moments through the plate. In general, these thermal moments force the plate to deflect. Only for some special cases, when the thermal moment vanishes for a thermal loading type or when the boundary conditions are capable of handling these extra moments, buckling may occur. Due to the asymmetrical mid-plane configuration of the plate, thermal moments do not omit for general cases of thermal loading (that are uniform temperature rise, linear temperature across the thickness/radial direction, tent-like thermal loading, and heat conduction across the thickness). Only for a special case of boundary conditions, and

that is the clamped one, the plate remains un-deformed in the pre-buckling state. The fact is that immovable clamping conditions are not influenced by the thermal loading. This conclusion which results from linear pre-buckling analysis is compatible with the result of Fallah and Nosier [31]. Therefore, this study covers FGM plates with clamped outer edge.

Also, the elastic foundation has no effect on the pre-buckling forces of the plate, because the pre-buckling state of the plate is free of deflection.

4 Stability equations

The adjacent equilibrium criterion may be used to obtain the stability equations of a circular-shaped plate [15–23,26]. For this purpose, assume an equilibrium position which is governed by the displacement components u_0^0, v_0^0, and w_0^0. The displacement components of a neighboring state of the stable equilibrium differ by u_0^1, v_0^1, and w_0^1 with respect to the equilibrium position. Thus, the total displacements of a neighboring state are [16–19]

$$u_0 = u_0^0 + u_0^1, \quad v_0 = v_0^0 + v_0^1, \quad w_0 = w_0^0 + w_0^1. \tag{14}$$

Note that in this study, $u_0^0 = v_0^0 = w_0^0 = 0$. Nonetheless, we present Eq. (14) in this form to present a general approach.

Similar to the displacements, the stress resultants are divided into two terms representing the stable equilibrium and the neighboring state. The stress resultants with superscript 1 are linear functions of displacement with superscript 1 [16]. Considering this, and using Eqs. (7) and (10), and performing proper simplifications, the stability equations become

$$\begin{aligned}
&N^1_{rr,r} + \frac{1}{r}N^1_{r\theta,\theta} + \frac{1}{r}(N^1_{rr} - N^1_{\theta\theta}) = 0,\\
&N^1_{r\theta,r} + \frac{2}{r}N^1_{r\theta} + \frac{1}{r}N^1_{\theta\theta,\theta} = 0,\\
&M^1_{rr,rr} + \frac{2}{r}M^1_{rr,r} + \frac{1}{r^2}M^1_{\theta\theta,\theta\theta} - \frac{1}{r}M^1_{\theta\theta,\theta} + \frac{2}{r}M^1_{r\theta,r\theta} + \frac{2}{r^2}M^1_{r\theta,\theta} + N^0_{rr}w^1_{0,rr} + N^0_{\theta\theta}\left(\frac{1}{r^2}w^1_{0,\theta\theta} + \frac{1}{r}w^1_{0,r}\right)\\
&\quad + 2N^0_{r\theta}\left(\frac{1}{r}w^1_{0,r\theta} - \frac{1}{r^2}w^1_{0,\theta}\right) - K_w w^1_0 H(r-b) = 0.
\end{aligned} \tag{15}$$

To obtain the stability equations in terms of the displacement components, Eq. (7) has to be inserted into the above equations. Upon substitution, second- and higher-order terms of incremental displacements may be omitted [16–19]. The resulting equations are three stability equations based on the classical plate theory for an FGM plate partially in contact with the Winkler elastic foundation:

$$\begin{aligned}
&E_1\left(u^1_{0,rr} + \frac{1}{r}u^1_{0,r} - \frac{1}{r^2}u^1_0 - \frac{1}{r^2}v^1_{0,\theta} + \frac{1}{r}v^1_{0,r\theta}\right) + \frac{(1-\nu)}{2}E_1\left(\frac{1}{r^2}u^1_{0,\theta\theta} - \frac{1}{r}v^1_{0,r\theta} - \frac{1}{r^2}v^1_{0,\theta}\right)\\
&\quad - E_2\left(w^1_{0,rrr} - \frac{1}{r^2}w^1_{0,r} + \frac{1}{r}w^1_{0,rr} - \frac{2}{r^3}w^1_{0,\theta\theta} + \frac{1}{r^2}w^1_{0,\theta\theta r}\right) = 0,\\
&E_1\left(\frac{1}{r^2}v^1_{0,\theta\theta} + \frac{1}{r}u^1_{0,r\theta} + \frac{1}{r^2}u^1_{0,\theta}\right) + \frac{(1-\nu)}{2}E_1\left(v^1_{0,rr} + \frac{1}{r}v^1_{0,r} - \frac{1}{r^2}v^1_0 + \frac{1}{r^2}u^1_{0,\theta} - \frac{1}{r}u^1_{0,r\theta}\right)\\
&\quad - E_2\left(\frac{1}{r}w^1_{0,rr\theta} + \frac{1}{r^2}w^1_{0,r\theta} + \frac{1}{r^3}w^1_{0,\theta\theta\theta}\right) = 0,\\
&\frac{E_2}{1-\nu^2}\left(u^1_{0,rrr} + \frac{2}{r}u^1_{0,rr} - \frac{1}{r^2}u^1_{0,r} - \frac{1}{r^3}u^1_0 + \frac{1}{r^3}u^1_{0,\theta\theta} + \frac{1}{r^2}u^1_{0,r\theta\theta} - \frac{1}{r^2}v^1_{0,r\theta} + \frac{1}{r^3}v^1_{0,\theta} + \frac{1}{r^3}v^1_{0,\theta\theta\theta}\right.\\
&\quad \left. + \frac{1}{r}v^1_{0,rr\theta}\right) - \frac{E_3}{1-\nu^2}\left(w^1_{0,rrrr} + \frac{2}{r}w^1_{0,rrr} - \frac{1}{r^2}w^1_{0,rr} + \frac{1}{r^3}w^1_{0,r} + \frac{2}{r^2}w^1_{0,rr\theta\theta} - \frac{2}{r^3}w^1_{0,r\theta\theta} + \frac{4}{r^4}w^1_{0,\theta\theta}\right.\\
&\quad \left. + \frac{1}{r^4}w^1_{0,\theta\theta\theta\theta}\right) + N^0_{rr}w^1_{0,rr} + N^0_{\theta\theta}\left(\frac{1}{r^2}w^1_{0,\theta\theta} + \frac{1}{r}w^1_{0,r}\right) + 2N^0_{r\theta}\left(\frac{1}{r}w^1_{0,r\theta} - \frac{1}{r^2}w^1_{0,\theta}\right) - K_w w^1_0 H(r-b) = 0.
\end{aligned} \tag{16}$$

Since the buckling state of the plate is the initiation of out-of-plane deformations, it is reasonable to uncouple the above-mentioned equations to obtain an equation in terms of only the out-of-plane displacement component. With some mathematical manipulations, one may obtain an uncoupled equation in terms of the incremental lateral displacement w_0^1. The uncoupling process is presented below:

1. The first of Eq. (16) is differentiated with respect to r.
2. The first of Eq. (16) is divided by r.
3. The second of Eq. (16) is differentiated with respect to θ and then divided by r.
4. The obtained equations in steps (1)–(3) are added and the result is multiplied by $\dfrac{E_2}{E_1(1-\nu^2)}$.
5. The obtained equation in step (4) is subtracted from the third of Eq. (16).

The resulting equation is an uncoupled equation in terms of w_0^1 obtained as

$$\begin{aligned} D_k\Big(&w^1_{0,rrrr}+\frac{2}{r}w^1_{0,rrr}-\frac{1}{r^2}w^1_{0,rr}+\frac{1}{r^3}w^1_{0,r}+\frac{2}{r^2}w^1_{0,rr\theta\theta}-\frac{2}{r^3}w^1_{0,r\theta\theta}\\ &+\frac{4}{r^4}w^1_{0,\theta\theta}+\frac{1}{r^4}w^1_{0,\theta\theta\theta\theta}\Big)-N^0_{rr}w^1_{0,rr}-N^0_{\theta\theta}\left(\frac{1}{r^2}w^1_{0,\theta\theta}+\frac{1}{r}w^1_{0,r}\right)\\ &-2N^0_{r\theta}\left(\frac{1}{r}w^1_{0,r\theta}-\frac{1}{r^2}w^1_{0,\theta}\right)+K_w w_0^1 H(r-b)=0, \end{aligned} \tag{17}$$

where $D_k=\dfrac{E_1E_3-E_2^2}{E_1(1-\nu^2)}$ is the equivalent flexural rigidity of an FG plate. As can be seen, D_0 and D_∞ are flexural rigidities of a plate made of ceramic and metal constituents, respectively. To reformulate the governing equations of a circular FGM plate based on first-order shear deformation plate theory, one may refer to Nosier and Fallah [32].

5 Solving the stability equation

In this section, an exact solution for the stability equation (17) is presented. Substituting pre-buckling forces from Eq. (12) into Eq. (17) gives us

$$\left\{\left(\frac{\partial^2}{\partial r^2}+\frac{1}{r}\frac{\partial}{\partial r}+\frac{1}{r^2}\frac{\partial^2}{\partial\theta^2}\right)\left(\frac{\partial^2}{\partial r^2}+\frac{1}{r}\frac{\partial}{\partial r}+\frac{1}{r^2}\frac{\partial^2}{\partial\theta^2}+\frac{N^T}{D_k}\right)+\frac{K_w}{D_k}H(r-b)\right\}w_0^1(r,\theta)=0. \tag{18}$$

It is more convenient to introduce the following non-dimensional parameters:

$$\bar r=\frac{r}{a},\quad \beta=\frac{b}{a},\quad \delta=\frac{h}{a},\quad k_w=\frac{K_w a^2}{D_0},\quad d=\frac{D_k}{D_0},\quad n^T=\frac{N^T a^2}{D_0}. \tag{19}$$

To obtain an exact solution, the plate is divided into two sections: in-contact and contact-less regions.

5.1 Interior region, in-contact domain

The interior domain of the plate is a solid circular plate on a foundation. The buckled shape of the plate, considering the asymmetric configurations and periodic conditions, has the following shape:

$$w_0^{1i}(a\bar r,\theta)=W_n^i(\bar r)\cos(n\theta), \tag{20}$$

where the superscript i indicates that the solution is associated to the interior domain. Also, n is the number of nodal diameters. Its positive values describe the asymmetrical buckling configuration, while for $n=0$, where the solution (20) is independent of the circumferential variable, symmetrical buckling is concluded. Substituting Eq. (20) into Eq. (18), with the simultaneous aid of the non-dimensional parameters (19), the following ordinary differential equation is obtained:

$$\left(\frac{d^2}{d\bar r^2}+\frac{1}{\bar r}\frac{d}{d\bar r}-\frac{n^2}{\bar r^2}+k_1^2\right)\left(\frac{d^2}{d\bar r^2}+\frac{1}{\bar r}\frac{d}{d\bar r}-\frac{n^2}{\bar r^2}+k_2^2\right)W_n^i(\bar r)=0. \tag{21}$$

The solution of this equation depends on k_1 and k_2 and should be classified as follows:

Case 1: $n^T > 2\sqrt{k_w d}$. In this case, the exact solution of the stability equation (21) can be found as

$$W_n^i(\bar{r}) = C_{1n} J_n(k_1\bar{r}) + C_{2n} J_n(k_2\bar{r}) + C_{3n} Y_n(k_1\bar{r}) + C_{4n} Y_n(k_2\bar{r}), \tag{22}$$

where

$$k_{1,2} = \sqrt{\frac{n^T \pm \sqrt{n^{T^2} - 4dk_w}}{2d}} \tag{23}$$

and J_n and Y_n stand for the Bessel functions of the first and second kind, respectively.
Case 2: $n^T = 2\sqrt{k_w d}$. For this case, the solution of the stability equation has the following exact solution:

$$W_n^i(\bar{r}) = C_{1n} J_n(k_1\bar{r}) + C_{2n}\bar{r} J_{n+1}(k_1\bar{r}) + C_{3n} Y_n(k_1\bar{r}) + C_{4n}\bar{r} Y_{n+1}(k_1\bar{r}), \tag{24}$$

where

$$k_1 = \sqrt{\frac{n^T}{2d}}. \tag{25}$$

Case 3: $n^T < 2\sqrt{k_w d}$. In such condition, the solution of the stability equation has the following explicit solution:

$$\begin{aligned} W_n^i(\bar{r}) = {} & C_{1n}\left(\frac{J_n(k_1\bar{r}) + J_n(k_2\bar{r})}{2}\right) + C_{2n}\left(\frac{J_n(k_1\bar{r}) - J_n(k_2\bar{r})}{2i}\right) \\ & + C_{3n}\left(\frac{Y_n(k_1\bar{r}) + Y_n(k_2\bar{r})}{2}\right) + C_{4n}\left(\frac{Y_n(k_1\bar{r}) - Y_n(k_2\bar{r})}{2i}\right), \end{aligned} \tag{26}$$

where

$$k_{1,2} = \sqrt{\frac{n^T \pm i\sqrt{4dk_w - n^{T^2}}}{2d}} \tag{27}$$

and i is the square root of -1. Note that, since the point $\bar{r} = 0$ is in the domain, both constants C_{3n} and C_{4n} have to be zero.

5.2 Exterior region, contact-less domain

This domain is an annular plate free to deflect. Recalling the stability equations (18), the following solution is adopted for this region:

$$w_0^{1o}(a\bar{r}, \theta) = W_n^o(\bar{r})\cos(n\theta), \tag{28}$$

where a superscript o shows that the discussions are about the exterior domain. Substituting Eq. (28) into the stability equation (18) yields a fourth-order differential equation in terms of $W_n^o(\bar{r})$, where its solution may be written as

$$W_n^o(\bar{r}) = C_{5n} J_n\left(\sqrt{\frac{n^T}{d}}\bar{r}\right) + C_{6n} Y_n\left(\sqrt{\frac{n^T}{d}}\bar{r}\right) + C_{7n}\bar{r}^n + C_{8n}\left\{\frac{Ln\bar{r}}{\bar{r}^{-n}}\right\}. \tag{29}$$

Note that the top form of the solution (29) is associated with symmetrical buckling ($n = 0$), while the lower solution presents the asymmetric buckling ($n > 0$).

5.3 Continuity and boundary conditions

The solution of the stability equation is accomplished when two out-of-plane boundary conditions on the outer edge and four continuity conditions on $\bar{r} = \beta$ are imposed into the associated equations.

5.3.1 Boundary conditions

As only a clamped circular plate results in a bifurcation point, slope and deflection of the outer edge ($r = a$) have to vanish. By means of the assumed solution (28), one arrives at

$$W_n^o(1) = \frac{\mathrm{d}W_n^o(1)}{\mathrm{d}\bar{r}} = 0. \tag{30}$$

5.3.2 Continuity conditions

At any point on $r = b$, we have a unified quantity for deflection, slope, normal moment, and shear. Therefore,

$$\begin{aligned} w_0^{1i} &= w_0^{1o}, \\ w_{0,r}^{1i} &= w_{0,r}^{1o}, \\ M_{rr}^{1i} &= M_{rr}^{1o}, \\ M_{rr,r}^{1i} + \frac{1}{b}M_{r\theta,\theta}^{1i} + \frac{1}{b}\left(M_{rr}^{1i} - M_{\theta\theta}^{1i}\right) - N^T w_{0,r}^{1i} &= M_{rr,r}^{1o} + \frac{1}{b}M_{r\theta,\theta}^{1o} + \frac{1}{b}\left(M_{rr}^{1o} - M_{\theta\theta}^{1o}\right) - N^T w_{0,r}^{1o}, \end{aligned} \tag{31}$$

where the last equality holds for the definition of the shear force according to the Kirchhoff plate theory considering the pre-buckling in-plane force effect. The two last continuity conditions contain the stretching-bending coupling effects. Since only the out-of-plane displacement is under solution, stretching-bending coupling effects should be dropped out of the two aforementioned conditions in a reasonable manner.

With the aid of Eqs. (20) and (28), the first and second conditions of Eq. (31) change to

$$\begin{aligned} W_n^i(\beta) &= W_n^o(\beta), \\ \frac{\mathrm{d}W_n^i(\beta)}{\mathrm{d}\bar{r}} &= \frac{\mathrm{d}W_n^o(\beta)}{\mathrm{d}\bar{r}}. \end{aligned} \tag{32}$$

The third condition, recalling the definition of linearized moment resultant along with the linearized in-plane force resultant, leads us to the following equality in $\bar{r} = \beta$:

$$\begin{aligned} E_1 F^i\left(u_0^1, v_0^1\right) - E_2 G^i\left(w_0^1\right) &= E_1 F^o\left(u_0^1, v_0^1\right) - E_2 G^o\left(w_0^1\right), \\ E_2 F^i\left(u_0^1, v_0^1\right) - E_3 G^i\left(w_0^1\right) &= E_2 F^o\left(u_0^1, v_0^1\right) - E_3 G^o\left(w_0^1\right), \end{aligned} \tag{33}$$

where we have set

$$\begin{aligned} F\left(u_0^1, v_0^1\right) &= u_{0,r}^1 + \frac{\nu}{b}v_{0,\theta}^1 + \frac{\nu}{b}u_0^1, \\ G\left(w_0^1\right) &= w_{0,rr}^1 + \frac{1}{b}w_{0,r}^1 + \frac{1}{b^2}w_{0,\theta\theta}^1. \end{aligned} \tag{34}$$

Also, a superscript on the functions F and G has to be transmitted to displacements u_0^1, v_0^1, and w_0^1.

As seen from Eq. (33), both functions F and G have to be continuous. From the continuity of $G(w_0^1)$, and with the simultaneous aid of Eqs. (20), (28), and (32), the following smoothness condition is gained:

$$\frac{d^2 W_n^i(\beta)}{\mathrm{d}\bar{r}^2} = \frac{d^2 W_n^o(\beta)}{\mathrm{d}\bar{r}^2}. \tag{35}$$

To gain the last condition in terms of W_n, the first stability equation and the fourth continuity condition are rewritten as

$$\begin{aligned} E_1 I^i\left(u_0^1, v_0^1\right) - E_2 L^i\left(w_0^1\right) &= E_1 I^o\left(u_0^1, v_0^1\right) - E_2 L^o\left(w_0^1\right) = 0, \\ E_2 I^i\left(u_0^1, v_0^1\right) - E_3 L^i\left(w_0^1\right) &= E_2 I^o\left(u_0^1, v_0^1\right) - E_3 L^o\left(w_0^1\right), \end{aligned} \tag{36}$$

where we have set

$$\begin{aligned} I(u_0^1, v_0^1) &= \left(u_{0,rr}^1 + \frac{1}{b}u_{0,r}^1 - \frac{1}{b^2}u_0^1 - \frac{1}{b^2}v_{0,\theta}^1 + \frac{1}{b}v_{0,r\theta}^1\right) + \frac{(1+\nu)}{2}\left(\frac{1}{b^2}u_{0,\theta\theta}^1 - \frac{1}{b}v_{0,r\theta}^1 - \frac{1}{b^2}v_{0,\theta}^1\right), \\ L(w_0^1) &= \left(w_{0,rrr}^1 - \frac{1}{b^2}w_{0,r}^1 + \frac{1}{b}w_{0,rr}^1 - \frac{2}{b^3}w_{0,\theta\theta}^1 + \frac{1}{b^2}w_{0,\theta\theta r}^1\right). \end{aligned} \tag{37}$$

Similarly, both functions L and I have to be continuous. Concurrent assist of Eqs. (20), (28), (32), and (35) leads us to

$$\frac{d^3 W_n^i(\beta)}{d\bar{r}^3} = \frac{d^3 W_n^o(\beta)}{d\bar{r}^3}. \tag{38}$$

Substituting the two boundary conditions (30) and four continuity conditions (32), (35), and (38) into Eqs. (22), (24), (26), and (29) provides a system of six linear homogeneous equations in terms of C_{pn}, $p = 1, 2, 5, 6, 7, 8$. As usual, the determinant of the coefficient matrix has to be set equal to zero to obtain a non-trivial solution. The smallest root of the determinantal equation, through the minimum positive roots of the buckling criteria equations, is the critical buckling load which is called n_{cr}^T. Note that, while the solution is exact, due to the classification of the solutions and complicated algebraic expression, presenting a closed form expression to estimate the critical buckling force is not easy.

Now, to obtain the critical buckling temperature, the temperature distribution through the plate should be known.

6 Types of thermal loading

6.1 Uniform temperature rise

A circular FG plate at reference temperature T_0 is assumed. When radial extension of the plate is prevented, temperature through the plate may be increased uniformly to $T = T_0 + \Delta T$ such that, at the onset of perturbation, bifurcation occurs. Substituting $T = T_0 + \Delta T$ into the fourth of Eq. (8) gives

$$N^T = \frac{\Delta T h}{1-\nu}\left(E_m\alpha_m + \frac{E_{cm}\alpha_m + E_m\alpha_{cm}}{k+1} + \frac{E_{cm}\alpha_{cm}}{2k+1}\right). \tag{39}$$

Using the definition of n_{cr}^T and solving for ΔT, the critical buckling temperature difference of the plate in this case is obtained as

$$\Delta T_{cr} = \frac{\delta^2}{12(1+\nu)} \times \frac{E_c}{P} n_{cr}^T \tag{40}$$

with

$$P = E_m\alpha_m + \frac{E_m\alpha_{cm} + E_{cm}\alpha_m}{k+1} + \frac{E_{cm}\alpha_{cm}}{2k+1}. \tag{41}$$

For an isotropic homogeneous circular plate k = 0 and Eq. (40) reduces to

$$\Delta T_{cr} = \frac{\delta^2}{12(1+\nu)\alpha_c} n_{cr}^T. \tag{42}$$

6.2 Linear temperature across the thickness

Consider a thin FGM circular plate where the temperatures at the ceramic-rich and metal-rich surfaces are T_c and T_m, respectively. The temperature distribution for the given boundary conditions is obtained by solving the heat conduction equation across the plate thickness. If the plate thickness is thin enough, as the first approximation, the temperature distribution is approximated linear through the thickness. So the temperature as a function of the thickness coordinate z may be written in the form

$$T = T_m + (T_c - T_m)\left(\frac{1}{2} + \frac{z}{h}\right). \tag{43}$$

Substituting Eq. (43) into Eq. (8) and solving for $\Delta T = T_c - T_m$ gives the critical buckling temperature difference between the metal-rich and ceramic-rich surfaces as

$$\Delta T_{cr} = \frac{\delta^2}{12(1+\nu)} \times \frac{E_c}{Q} n_{cr}^T - (T_m - T_0)\frac{P}{Q}, \tag{44}$$

where P is defined by Eq. (41) and Q is equal to

$$Q = \frac{E_m \alpha_m}{2} + \frac{E_m \alpha_{cm} + E_{cm} \alpha_m}{k+2} + \frac{E_{cm} \alpha_{cm}}{2k+2}. \tag{45}$$

For an isotropic homogeneous circular plate $k = 0$, and Eq. (44) reduces to

$$\Delta T_{cr} = \frac{\delta^2}{6(1+\nu)\alpha_c} n_{cr}^T - 2(T_m - T_0). \tag{46}$$

6.3 Nonlinear temperature through the thickness

Assume an FGM circular plate where the temperature in ceramic-rich and metal-rich surfaces is T_c and T_m, respectively. The governing equation for the steady-state 1-D heat conduction equation, in the absence of heat generation, becomes

$$\begin{gathered} \frac{d}{\mathrm{d}z}\left(K(z)\frac{\mathrm{d}T}{\mathrm{d}z}\right) = 0, \\ T\left(\frac{h}{2}\right) = T_c, \quad T\left(-\frac{h}{2}\right) = T_m. \end{gathered} \tag{47}$$

Solving this equation via the polynomial series and taking the sufficient terms yield the temperature distribution across the thickness of the plate. Following the same method used for the linear temperature type, the critical buckling temperature difference between the upper and lower surfaces of the plate may be evaluated as

$$\Delta T_{cr} = \frac{\delta^2}{12(1+\nu)} \times \frac{E_c}{R} n_{cr}^T - (T_m - T_0)\frac{P}{R} \tag{48}$$

with the following definitions:

Table 1 Material properties of aluminum and alumina as constituents of the FGM circular plate

Property	Aluminum (Al)	Alumina (Al_2O_3)
E (GPa)	70	380
K (W/mK)	204	10.4
$\alpha(1/K)$	23×10^{-6}	7.4×10^{-6}
ν	0.3	0.3

$$
\begin{aligned}
D &= \sum_{i=0}^{N} \frac{\left(-\frac{K_{cm}}{K_m}\right)^i}{ik+1}, \\
R &= \frac{1}{D} \times \left\{ E_m \alpha_m \sum_{i=0}^{N} \frac{\left(-\frac{K_{cm}}{K_m}\right)^i}{(ik+1)(ik+2)} + (E_{cm}\alpha_m + E_m \alpha_{cm}) \sum_{i=0}^{N} \frac{\left(-\frac{K_{cm}}{K_m}\right)^i}{(ik+1)(ik+k+2)} \right. \\
&\quad \left. + E_{cm}\alpha_{cm} \sum_{i=0}^{N} \frac{\left(-\frac{K_{cm}}{K_m}\right)^i}{(ik+1)(ik+2k+2)} \right\},
\end{aligned} \tag{49}
$$

where N, the number of expanded terms, should be chosen to assure the convergence of the series.

For an isotropic homogeneous plate k = 0, and expression (48) simplifies to

$$
\Delta T_{cr} = \frac{\delta^2}{6(1+\nu)\alpha_c} n_{cr}^T - 2(T_m - T_0), \tag{50}
$$

which is similar to Eq. (46), since the solution of the heat conduction equation (47) is linear across the thickness when the thermal conductivity of the plate is position independent.

7 Results and discussion

To illustrate the proposed approach, a ceramic–metal functionally graded circular plate is considered. The combination of materials consists of aluminum and alumina. The plate is assumed to be clamped at the outer edge. The material properties are graded across the thickness. For each constituent, the thermomechanical properties are given in Table 1.

To show the validity and accuracy of the present method, the non-dimensional critical buckling force of a homogeneous foundation-less plate is compared with those reported in [16] and [23]. In our study, when $k_w = \beta = 10^{-10}$ are assumed, $n^T = 14.6820$ is gained which is the same as reported in [16] based on an exact analysis and the available result in [23] based on the Chebyshev polynomial series solution.

The critical buckling force of isotropic homogeneous plates ($k = 0$) for various values of k_w and β is presented in Table 2. As observed in this table, while the value of Winkler constant increases the thermal buckling force becomes larger, which is due to the resistance of the elastic foundation against the deflection of the plate. Some interesting behaviors are observed through the results. Note that a partial elastic foundation may change the number of nodal diameters, while this change may be of an increasing type or decreasing type. It is worth mentioning that as loading type is symmetric, in many cases the buckling configuration of the plate is asymmetric which proves the necessitation of the asymmetrical eigenvalue analysis of the buckling problem under the action of symmetrical loading. As the constant β increases, n_{cr}^T increases permanently, since a larger domain is adopted to resist against the deformation of the plate. Furthermore, for each constant of k_w, the effect of foundation radii on the number of nodal points is not monotonic. As apparent, the number of nodal points is constant and equal to zero for $k_w = 16$. For $k_w = 256$, an increase in the number of nodal points is observed. A fluctuation exists for n when the Winkler foundation constant is $k_w = 4{,}096$.

Some buckled configurations of an FGM plate ($k = 0.5$), located on a partial Winkler elastic foundation with foundation radii $\beta = 0.5$, are shown in Fig. 2. As can be seen, for foundation-less condition, the plate

Table 2 Non-dimensional critical thermal force n_{cr}^{T} of isotropic homogeneous circular plates on a partial Winkler elastic foundation

β	$k_w = 0$	$k_w = 2^4$	$k_w = 4^4$	$k_w = 6^4$	$k_w = 8^4$
0.0	14.682^0	14.682^0	14.682^0	14.682^0	14.682^0
0.1	14.682^0	14.811^0	16.713^0	24.262^0	26.905^1
0.2	14.682^0	15.158^0	22.062^0	28.676^1	32.647^1
0.3	14.682^0	15.625^0	28.351^1	35.239^1	44.951^2
0.4	14.682^0	16.092^0	31.141^1	46.554^2	55.293^2
0.5	14.682^0	16.464^0	34.739^1	55.103^2	73.197^3
0.6	14.682^0	16.697^0	37.984^1	67.187^2	94.167^3
0.7	14.682^0	16.807^0	39.868^1	76.996^0	124.265^1
0.8	14.682^0	16.843^0	40.513^1	79.941^0	135.792^1
0.9	14.682^0	16.848^0	40.614^1	80.418^0	137.043^1
1.0	14.682^0	16.851^0	40.617^1	80.425^0	138.459^1

Numbers of nodal diameters are shown as superscript

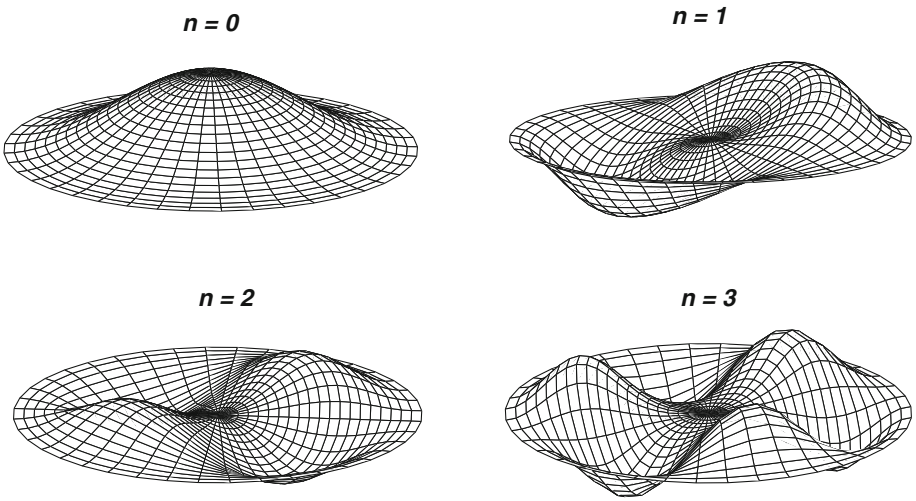

Fig. 2 Influence of Winkler elastic foundation on buckled shape of a partially supported ($\beta = 0.5$) FGM plate ($k = 0.5$)

buckles in a symmetrical manner, where the peak deflection is at the center. Note that since the deformation is symmetric, the slope at the center point of the plate vanishes. In this case, the buckling load is the smallest positive root of the equation $J_1(1.242\sqrt{n_{cr}^{T}}) = 0$, which is $n_{cr}^{T} = 9.517$. The symmetric shape of the plate persists as long as $k_w < 99$. As the Winkler constant stands in the range $99 < k_w < 466$, the number of nodal diameters increases up to one and asymmetrical shapes are observed. In this domain, the peak deflection of the plate moves toward the edge of the plate. The asymmetrical shape of the plate persists when k_w increases from 466, while the number of nodal diameters also increases up to 2. This configuration is persistent as long as a Winkler foundation with $k_w < 2{,}305$ acts against the deflection. For $k_w > 2{,}305$, the buckled shapes are asymmetric where the lowest critical load of the plate is associated with $n = 3$. For instance, the first four buckling configurations ($n = 1, 2, 3, 4$) are depicted in Fig. 2 which are associated to a foundation with stiffness $k_w = 0, 200, 2{,}000, 4{,}000$, respectively. Consequently, the associated non-dimensional loads are $n_{cr}^{T} = 9.517, 24.806, 44.764, 50.734$.

The critical buckling temperatures of an FGM circular plate, when the complete surface of the plate is attached to the foundation, are given in Table 3. Three cases of ΔT_{cr} are considered. Various power law indexes ($k = 0, 0.5, 1, 2, 5, \infty$) and various foundation coefficients are considered. For linear and nonlinear temperature distribution cases (LTD and NLTD, respectively), a $5K$ increase in the metal rich surface is assumed, that is, $T_m - T_0 = 5K$. An interesting behavior is observed for $k_w = 500$ where the number of nodal points fluctuates when the power law index becomes larger. The LTD case, as the most simple approximation of NLTD, always underrates the critical buckling temperature except for the cases of $k = 0, \infty$, when an FGM plate reduces to a homogeneous one made of its constituents. Note that while the Winkler elastic foundation

Table 3 Critical buckling temperature difference $\Delta T_{cr}[K]$ of FGM circular plates ($\delta = 0.015$) subjected to different types of thermal loading over a complete elastic foundation

k_w	Load type	$k = 0$	$k = 0.5$	$k = 1$	$k = 2$	$k = 5$	$k = \infty$
	UTR	28.616^0	16.213^0	13.294^0	11.786^0	12.159^0	9.207^0
0	LTD	47.232^0	22.433^0	15.556^0	11.946^0	12.324^0	8.414^0
	NLTD	47.232^0	39.045^0	27.652^0	19.913^0	17.359^0	8.414^0
	UTR	53.896^0	37.465^0	34.044^1	32.654^1	35.781^1	34.833^1
100	LTD	97.793^0	64.950^0	54.470^1	48.681^1	52.984^1	59.640^1
	NLTD	97.793^0	113.047^0	96.830^1	81.149^1	74.631^1	59.640^1
	UTR	109.811^1	72.229^0	65.424^0	64.339^0	71.595^0	72.019^1
500	LTD	198.051^1	134.497^0	113.323^0	104.457^0	114.630^0	132.169^1
	NLTD	198.051^1	234.096^0	201.450^0	174.126^0	161.464^0	132.169^1
	UTR	140.651^0	96.118^0	89.470^0	89.761^1	100.480^1	98.478^0
1,000	LTD	271.302^0	182.288^0	158.421^0	149.700^1	161.278^1	186.957^0
	NLTD	271.302^0	317.279^0	281.619^0	246.211^1	227.171^1	186.957^0
	UTR	192.288^0	132.471^1	122.876^1	123.100^0	136.811^0	136.738^1
2,000	LTD	374.577^0	255.017^1	221.072^1	207.896^0	226.886^0	263.476^1
	NLTD	374.577^0	443.865^1	392.993^1	346.556^0	319.585^0	263.476^1
	UTR	294.896^1	203.780^0	190.131^0	189.366^1	211.828^1	212.457^0
5,000	LTD	579.791^1	397.676^0	347.207^0	324.546^1	356.011^1	414.914^0
	NLTD	579.791^1	682.168^0	617.217^0	541.007^1	501.467^1	414.914^0

Numbers of nodal diameters are shown as superscript

postpones the branching point of the plate, this effect may be compensated with the composition rule of the constituents.

The first four buckled configurations of a homogeneous circular plate over a complete elastic foundation are depicted in Fig. 3. Starting from a foundation-less plate, it is seen that the plate exhibits a symmetrical buckled shape ($n = 0$) and this persists until $k_w < 177$. In this case, the peak deflection of the plate is at the center point, and due to the symmetric configuration, the slope vanishes at the center. In the range $176 < k_w < 723$, the plate buckles in an asymmetrical shape when the number of nodal diameters is equal to one. In the mentioned range, the center deflection is equal to zero. In the third domain $722 < k_w < 2{,}283$, again, symmetrical buckling exists. Peak deflection stands at the center, the same as in the first region. The major difference between this region and the first one is the existence of a ring without deflection. The fourth region covers the range $2{,}282 < k_w < 5{,}095$. In this domain, the same as the second one, asymmetrical shapes are distinguished. The existence of one un-deflected point on each radial line is the only difference between the schematic of fourth and second domains. When the Winkler constant becomes larger than 5,094, again, buckling without nodal points occurs. Configurations are in a way that each radial line of the plate consists of two un-deflected points. Similar to the results reported in [7], for the mechanical buckling of isotropic homogeneous plates, within the studied domain, no buckling is observed for $n > 1$. For sufficiently stiff Winkler foundation, however, it may occur [7]. It is worth noting that the mode transition of fully supported circular plates is totally different from that which occurs in a partially supported plate, as stated in the discussions of Fig. 2.

8 Conclusion

To demonstrate the effects of thickness, foundation radii, power law index, elastic foundation coefficients, and loading type, an analytical method is presented for the accurate prediction of critical buckling temperature differences as well as buckled shapes of heated circular FG plates. The derivation of equations is based on the classical plate theory, while the constituent materials follow a power law form of property distribution. A circular plate with immovable clamped boundary condition is considered. An eigenvalue analysis of the stability equations is presented, and analytical expressions are derived for the critical buckling temperatures. It is concluded that:

1. For a transversely graded FGM circular plate with or without (complete or partial) Winkler elastic foundation restrained from thermal expansion, thermally induced bifurcation occurs only for a clamped one. For FGM plates with hard simply supported edge or extensionally fixed free edge, the plate exhibits a lateral deflection with the onset of thermal load. Considering the occurrence of primary–secondary equilibrium paths for these two later cases is quantitatively wrong.

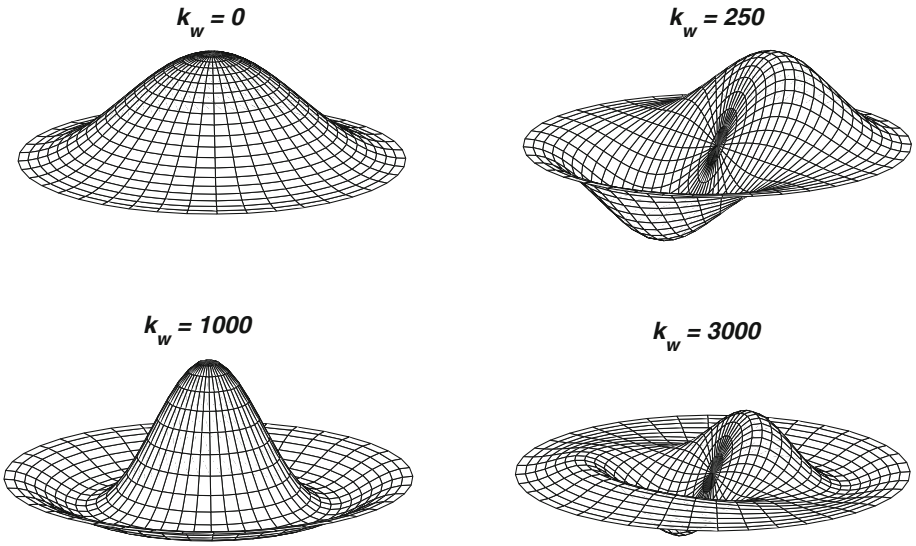

Fig. 3 Influence of foundation coefficient on buckled configuration of homogeneous plate over a complete Winkler elastic foundation (figures are schematically shown and are not normalized)

2. For a contact-less circular FG plate, the thermal buckled shape is symmetric, while in some cases buckled configurations of partially in-contact clamped FG plates may be asymmetric with non-zero nodal points. Therefore, when the stability equations are solved independent of the variable θ, ΔT_{cr} is over-estimated and the buckled shape of the plate is predicted wrongly.
3. For a completely supported plate, the number of nodal diameters with the increase of Winkler stiffness fluctuates between 0 and 1, permanently, while ΔT_{cr} increases monotonically when k_w becomes larger.
4. For contact-less plates, the buckled configuration of a plate is independent of the power law index, while for partially/completely in-contact plates, the power law index may change the number of nodal diameters in some cases.

References

1. Wang, C.M., Xiang, Y., Kitipornchai, S., Liew, K.M.: Axisymmetric buckling of circular Mindlin plates with ring supports. J. Struct. Eng. **119**(3), 782–793 (1993)
2. Wang, C.M., Xiang, Y., Wang, Q.: Axisymmetric buckling of Reddy circular plates on Pasternak foundation. J. Eng. Mech. **127**(3), 254–259 (2001)
3. Wang, C.M., Aung, T.M.: Buckling of circular Mindlin plates with an internal ring support and elastically restrained edge. J. Eng. Mech. **131**(4), 359–366 (2005)
4. Wang, C.M., Wang, C.Y.: Buckling of circular plates with an internal ring support and elastically restrained edges. Thin-Walled Struct. **39**(9), 821–825 (2001)
5. Yu, L.H., Wang, C.Y.: Buckling mosaic of concentrically hinged or cracked circular plates on elastic foundation. AIAA J. **47**(9), 2253–2255 (2009)
6. Yu, L.H., Wang, C.Y.: Buckling mosaic of a circular plate on a partial elastic foundation. Struct. Eng. Mech. **34**(1), 135–138 (2010)
7. Wang, C.Y.: On the buckling of a circular plate on an elastic foundation. J. Appl. Mech. **72**(5), 795–796 (2005)
8. Rao, L.B., Rao, C.K.: Buckling of circular plates with an internal elastic ring support and elastically restrained guided edge. Mech. Based Des. Struct. Mach. **37**(1), 60–72 (2009)
9. Rao, L.B., Rao, C.K.: Buckling analysis of circular plates with elastically restrained edges and resting on internal elastic ring support. Mech. Based Des. Struct. Mach. **38**(4), 440–452 (2010)
10. Wang, A.: Axisymmetric postbuckling and secondary bifurcation buckling of circular plates. Int. J. Non-Linear Mech. **35**(2), 279–292 (2000)
11. Ma, L.S., Wang, T.J.: Thermal postbuckling and bending behavior of circular plates with temperature dependent material properties. Key Eng. Mater. **243–244**, 195–200 (2003)
12. Li, S.-R., Batra, R.C., Ma, L.S.: Vibration of thermally post-buckled orthotropic circular plates. J. Therm. Stress. **30**(1), 43–57 (2007)
13. Rao, G.V., Varma, R.R.: Simple formulation to predict thermal postbuckling load of circular plates. AIAA J. **45**(7), 1784–1786 (2007)
14. Ramaraju, R.V., Gundabathula, V.R.: Reinvestigation of intuitive approach for thermal postbuckling of circular plates. AIAA J. **47**(10), 2493–2495 (2009)

15. Najafizadeh, M.M., Eslami, M.R.: Buckling Analysis of Circular plates of functionally graded materials under uniform radial compression. Int. J. Mech. Sci. **44**(12), 2479–2493 (2002)
16. Najafizadeh, M.M., Eslami, M.R.: First-order-theory-based thermoelastic stability of functionally graded material circular plates. AIAA J. **40**(7), 1444–1450 (2002)
17. Najafizadeh, M.M., Heydari, H.R.: An exact solution for buckling of functionally graded circular plates based on higher order shear deformation plate theory under uniform radial compression. Int. J. Mech. Sci. **50**(3), 603–612 (2008)
18. Najafizadeh, M.M., Heydari, H.R.: Thermal buckling of functionally graded circular plates based on higher order shear deformation plate theory. Eur. J. Mech. A Solids **23**(6), 1085–1100 (2004)
19. Naderi, A., Saidi, A.R.: An analytical solution for buckling of moderately thick functionally graded sector and annular sector plates. Arch. Appl. Mech. **81**(6), 809–828 (2011)
20. Naderi, A., Saidi, A.R.: Buckling analysis of functionally graded annular sector plates resting on elastic foundations. ImechE Part C **225**(2), 312–325 (2011)
21. Naderi, A., Saidi, A.R.: Exact solution for stability analysis of moderately thick functionally graded sector plates on elastic foundation. Compos. Struct. **93**(2), 629–638 (2011)
22. Saidi, A.R., Hasani Baferani, A.: Thermal buckling analysis of moderately thick functionally graded annular sector plates. Compos. Struct. **92**(7), 1744–1752 (2010)
23. Jalali, S.K., Naei, M.H., Poorsolhjouy, A.: Thermal stability analysis of circular functionally graded sandwich plates of variable thickness using pseudo-spectral method. Mater. Des. **31**(10), 4755–4763 (2010)
24. Ma, L.S., Wang, T.J.: Nonlinear bending and post-buckling of a functionally graded circular plate under mechanical and thermal loadings. Int. J. Solid Struct. **40**(13–14), 3311–3330 (2003)
25. Ma, L.S., Wang, T.J.: Buckling of functionally graded circular/annular plates based on the first-order shear deformation plate theory. Key Eng. Mater. **261–263**, 609–614 (2004)
26. Sepahi, O., Forouzan, M.R., Malekzadeh, P.: Thermal buckling and postbuckling analysis of functionally graded annular plates with temperature-dependent material properties. Mater. Des. **32**(7), 4030–4041 (2011)
27. Li, S.R., Zhang, J.H., Zhao, Y.G.: Nonlinear thermomechanical post-buckling of circular fgm plate with geometric imperfection. Thin-Walled Struct. **45**(5), 528–536 (2007)
28. Hetnarski, R.B., Eslami, M.R.: Thermal stresses: advanced theory and applications. In: Solid Mechanics and its Applications, vol. 158. Springer, Berlin (2008)
29. Reddy, J.N.: Mechanics of Laminated Composite Plates and Shells: Theory and Analysis. CRC Press, Boca Raton (2004)
30. Tauchert, T.R.: Thermal buckling of thick antisymmetric angle-ply laminates. J. Therm. Stress. **10**(2), 113–124 (1987)
31. Fallah, F., Nosier, A.: Nonlinear behavior of functionally graded circular plates with various boundary supports under assymetric thermo-mechanical loading. Compos. Struct. **94**(9), 2834–2850 (2012)
32. Nosier, A., Fallah, F.: Reformulation of Mindlin–Reissner governing equations of functionally graded circular plates. Acta Mech. **198**(3–4), 209–233 (2008)